Journal of Power Sources 215 (2012) 11–17

Contents lists available at SciVerse ScienceDirect

Journal of Power Sources

journal homepage: www.elsevier.com/locate/jpowsour

Separate *in situ* measurements of ECA under land and channel in PEM fuel cells

Andrew Higier [1], Hongtan Liu*

Clean Energy Research Institute, College of Engineering, University of Miami, Coral Gables, FL 33146, USA

HIGHLIGHTS

- ECAs under the land and channel areas in a PEMFC were measured.
- ECA under the land area is higher due to direct compression.
- ECA is the most important factor in local current density.
- ECA increases with compression.
- True concentration loss for the land is greater than known before.

ARTICLE INFO

Article history:
Received 15 February 2012
Received in revised form
27 April 2012
Accepted 29 April 2012
Available online 4 May 2012

Keywords:
PEM fuel cells
Electrochemical area
GDL compression
Cyclic voltammetry

ABSTRACT

Separate *in situ* measurements of electrochemical areas (ECA) under land and channel areas in proton exchange membrane (PEM) fuel cells are realized using cyclic voltammetry. Experiments are carried out using special membrane electrode assemblies (MEA) in single-channel serpentine flow fields with different widths of channels and lands. The experimental results show that ECAs are significantly higher in the areas under the land than that under the channel. ECA-normalized polarization curves show that ECA is the most significant factor causing higher current density under the land than under the channel in the high cell potential region, and the true concentration polarization under the land in the low potential region is actually much greater than what can be seen in conventional polarization curves. Further experimental results show that, within the compression pressure range examined, ECA increases with compression pressure significantly.

1. Introduction

In a PEM fuel cell, current density under the land and channel areas can vary significantly and many early modeling studies indicated that current density under the land areas were much lower than that under the channel [1–4], mainly due to the higher mass transfer resistance under the land area. However, indirect measurement results by Freunberger et al. [5] showed that current density could actually be higher under the land than under the channel. Direct measurements by Wang and Liu [6] showed that the current density was higher under the land in a parallel flow field in the high cell potential region and that the lateral resistance of the gas diffusion layer (GDL) was not a significant factor. Further direct measurements [7] found that the current density in a serpentine flow field is also higher under the land than under the channel in typical cell operating potential regions. A follow up study found that this trend is common for a variety of serpentine flow field dimensions [8]. Further study has shown that lower total electrical resistance under the land area due to direct compression from the flow plate structure is an important factor causing the higher local current density under the land at the high cell voltage region [9].

However, upon closer examinations of the polarization curves [e.g. 6–9] one can find that the current density was higher under the land even at very low current densities. In this region, ohmic losses are not significant, thus, though the difference in total electrical resistance is an important factor, it cannot be the only factor that causes the higher local current density under the land areas. In addition, it is well known that in the low current density region, concentration losses are negligible. Since both the areas under the land and under the channel operate at very similar, if not identical, temperature and pressure, there is no significant difference in the electrochemical kinetics—the exchange current density can be assumed to be the same for the two areas. After eliminating the various factors discussed above, only one factor is left unexamined, the local electrochemical active area (ECA). Only a difference in local ECAs between the areas under the land and the channel can cause such a significant difference in current density

* Corresponding author. Tel.: +1 305 284 2019; fax: +1 305 284 2580.
E-mail address: hliu@miami.edu (H. Liu).
[1] Present address: Applied Research Center, Florida International University, Miami, FL, USA.

0378-7753/$ – see front matter © 2012 Elsevier B.V. All rights reserved.
doi:10.1016/j.jpowsour.2012.04.098

at the very low current density region. Thus, the objective of this study is to separately measure the ECAs under the land and under the channel *in situ* to determine if there is a difference and if so to determine what effect this difference has on performance and finally to determine the cause for such a difference.

2. Experimental methodology

2.1. In situ cyclic voltammetry

In this study, in order to separately measure ECAs under the different areas, an *in situ* cyclic voltammetry technique is used. Cyclic voltammetry is one of the most widely used techniques in studies of electrochemical cells. The general procedure is to place an electrode to be studied in contact with an electrolyte, the potential is then swept forward and backward over a voltage range in which surface adsorption/desorption reactions occur. In this manner, the number of reactive surface sites can be obtained by recording the total charge required for monolayer adsorption/desorption [10]. This technique may be used in PEMFC to determine the H_2 adsorption charge. The technique involves measuring the electro-adsorption and desorption of hydrogen onto platinum. The forward sweep causes desorption of hydrogen and the reverse sweep causes the adsorption on to the Pt surface. The technique was also described by Wu et al. [11], where they calculated the ECA using the H_2 adsorption charge determined from the adsorption area of the cyclic voltammetry plot. This particular method of calculating the ECA for a PEMFC was originally described by Ralph et al. [12] while investigating low cost electrodes for PEMFC. In addition, Folgado et al. conducted a study and found that adsorption and desorption charges are strongly dependent on sweep rate voltage and temperature [13]. Schneider et al. utilized a segmented microstructure flow field in order to conduct cyclic voltammetry tests throughout the flow field [14].

The fuel cell test system and the fuel cell fixture used in this study are the same as in previous studies [6–9]. In a similar manner to those previous studies the experiments were conducted separately under the land and under the channel. The two areas were isolated in a manner shown in Fig. 1(a) and (b) below.

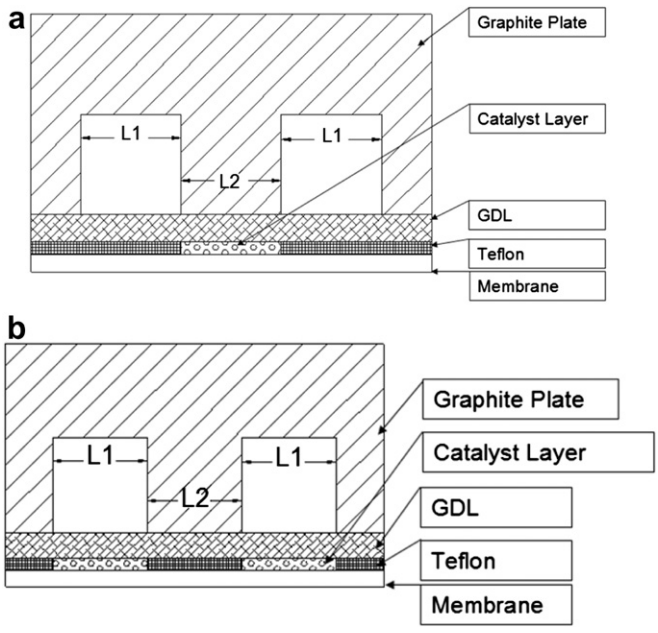

Fig. 1. (a) Experimental fuel cell for determining ECA under the land area. (b) Experimental fuel cell for determining ECA under the channel area.

Table 1
Flow field land and channel dimensions used in the cyclic voltammetry experiments.

Design	L1 (mm)	L2 (mm)
A	2	3
B	2	2
C	1	1

In order to measure the ECA of the land area, the catalyst under the channel is completely removed and the area is electrically insulated by a layer of Teflon® the same thickness as the catalyst layer. The reverse is true when measuring the ECA under the channel area. The experiments were conducted using various serpentine flow fields with different land and channel width dimensions. The flow field used is a single-channel and single-pass serpentine flow field with 2 channels and 1 land. Three different flow field designs used are shown in Table 1.

In order to minimize any effect of the anode side, a full flow field with a 50 cm^2 MEA in the anode is used. The schematics of the MEAs used in both cathode and anode sides as well as the cathode flow field are shown in Fig. 2.

The membrane used in the fuel cell was Nafion® 117 from Alfa-Aesar. The electrodes for the anode and cathode sides were provided by BCS Fuel Cells. The catalyst loading was 0.4 mg cm^{-2}. The MEAs were assembled and hot pressed in house.

The cyclic voltammetry tests were run using a Princeton Applied Research Versastat 3 Potentiostat. The anode and cathode humidification temperatures as well as the cell temperature were 35 °C for all the experiments, unless specified otherwise. The experiments were conducted *in situ* using a two-electrode configuration, where one side of the cell acts as both the reference and counter electrodes and the other side works as the working electrode. In this case the cathode side is the working electrode and the anode serves as the reference and counter electrodes. In order to perform the cyclic voltammetry experiments, nitrogen gas is fed into the cathode (working electrode) and pure hydrogen is fed into the anode (counter/reference electrode). The cathode flow rate changes for different experiments but the hydrogen flow rate is kept constant at 0.2 L min^{-1}. The voltage is then swept forward and backward between 0.01 and 1.0 V at a scan rate of 2.0 mV s^{-1}. The entire potential sweep was repeated 3 times for each experiment. During the reverse sweep proton reduction to adsorption occurs and the hydrogen adsorption charge density can be determined. The ECA is calculated using the following equation:

$$\mathrm{ECA} = \frac{q}{\Gamma \cdot L}, \tag{1}$$

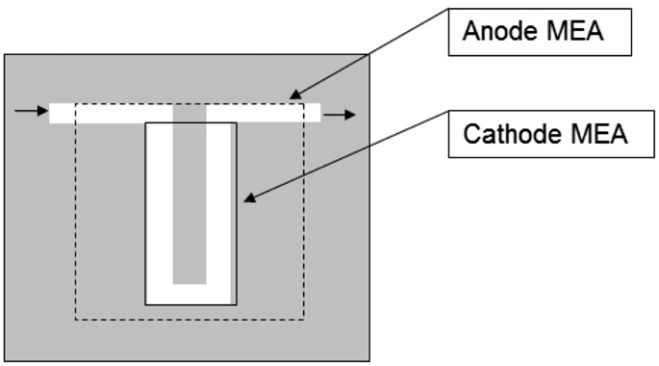

Fig. 2. Schematics of cathode serpentine flow field and both the anode and cathode MEAs. The anode MEA is a full 50 cm^2 while the cathode MEA is a smaller specialized area. The dotted line represents the relative size of the anode MEA as compared to that of the cathode.

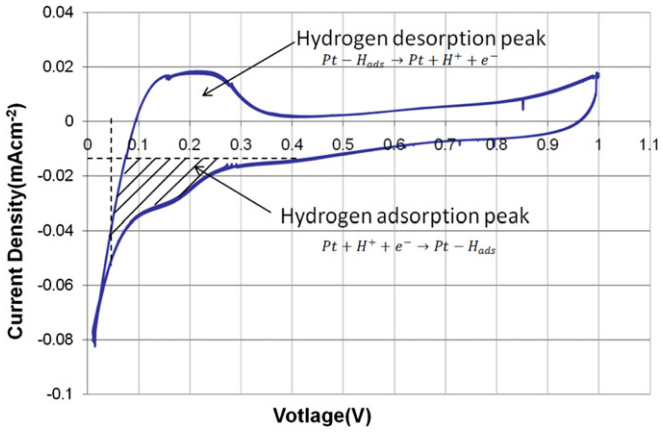

Fig. 3. A sample cyclic voltammogram showing the desorption/adsorption peaks and the area under which the adsorption charge density is determined.

where q is the adsorption charge density(C cm^{-2}), L is the manufacturer catalyst loading (g cm^{-2}) and Γ is a constant for the charge to reduce a monolayer of protons onto Pt for a smooth catalyst, the value used is 210 μC cm^{-2} Pt [15].

Fig. 3 displays a sample cyclic voltammogram and describes the hydrogen adsorption and desorption peaks. The adsorption charge density is determined by integrating the area under the curve, shown in the shaded region.

2.2. ECA under different compressions

In order to determine if the difference in ECA under the land and channel is caused by the fact that the area under the channel experiences less compression than that under the land [16,17] additional experiments were conducted in order to measure ECA as a function of cell compression. In order to accomplish this, a specially designed fuel cell, designed and manufactured in house, was used. The cell allows the user to vary and measure the amount of compression of the gas diffusion electrode (GDE). The cell setup was similar to that used in ref. [18] and is designed to allow direct measurement of overall GDE compression. The experiments were conducted on a 2 mm land using the experimental setup described in Section 2.1. In this manner the cell was compressed to 10% from its original thickness and the ECA was measured. The tests were repeated in increments of approximately 5% compression up until approximately 25%.

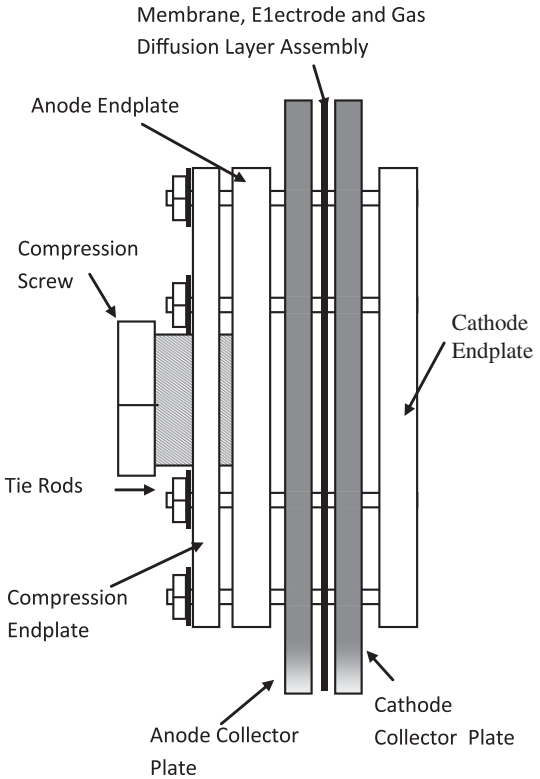

Fig. 4. Schematic of fuel cell assembly used in measurement of ECA as functions of compression.

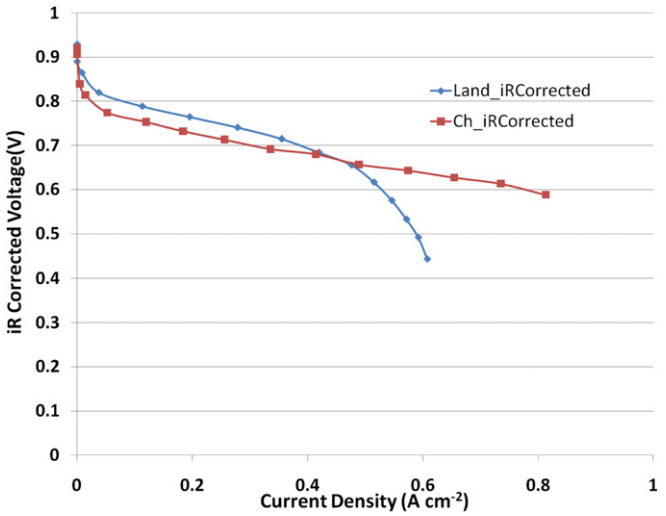

Fig. 5. iR-corrected polarization curve for 2 mm land and 2 mm channel. Cathode reactant is air; pressure is atmospheric.

3. Experimental results and discussion

3.1. iR-corrected polarization curves

In ref. [8] it was found that the difference in total electronic resistance between the land and channel areas is an important

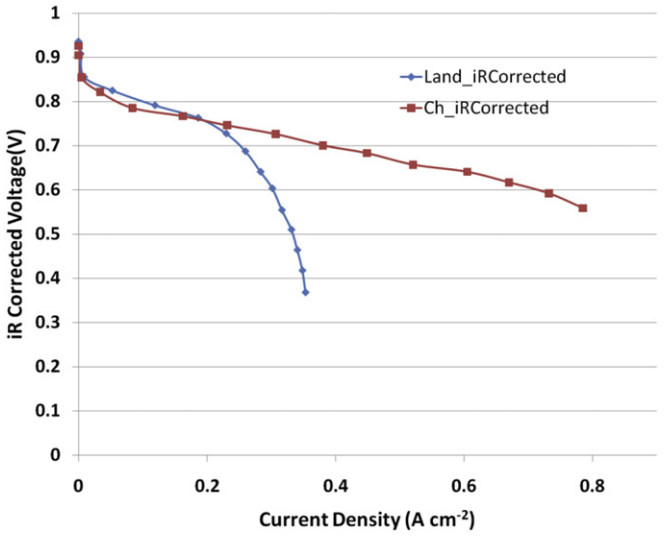

Fig. 6. iR-corrected polarization curve for 3 mm land and 2 mm channel. Cathode reactant is air; pressure is atmospheric.

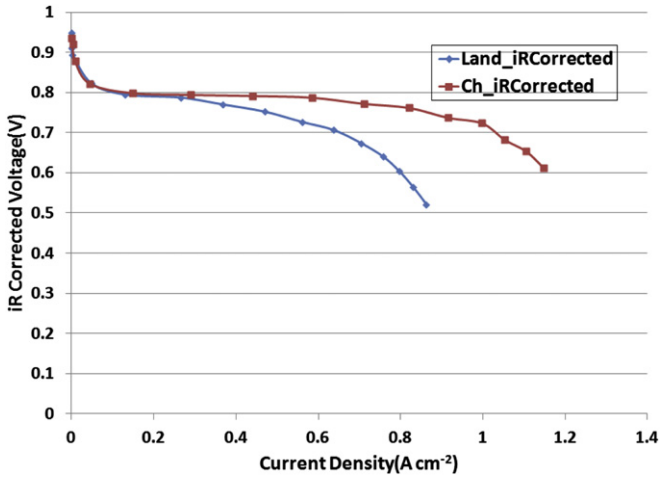

Fig. 7. iR-corrected polarization curve for 1 mm land and 1 mm channel. Cathode reactant is air; pressure is atmospheric.

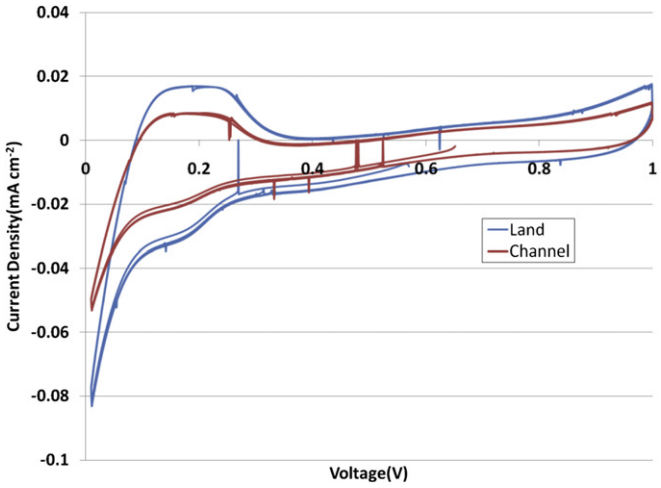

Fig. 9. Cyclic voltammetry results for 2 mm land and 2 mm channel. The nitrogen purge rate is 200 sccm and the hydrogen flow rate is 200 sccm.

factor for the different local current densities observed. To determine if the difference in electronic resistance is the only major factor comparison of iR-corrected polarization curves of land and channel areas can be made. The ohmic loss in a fuel cell is given by $\eta_{ohmic} = I \bullet \mathrm{ASR}$, where ASR is the area-specific resistance. At any given current density the ohmic losses for the land and channel areas can be calculated as:

Land:

$$\eta_{ohmic} = i\left(\mathrm{ASR}_{ion} + \mathrm{ASR}_{ele}^{ld}\right). \quad (2)$$

Channel:

$$\eta_{ohmic} = i\left(\mathrm{ASR}_{ion} + \mathrm{ASR}_{ele}^{ch}\right). \quad (3)$$

The iR-corrected voltage is obtained as follows:

$$V_{corrected} = V + \eta_{ohmic}, \quad (4)$$

where i is the current density, ASR_{ion} is the area-specific ionic resistance of the membrane, ASR_{ele}^{ld} and ASR_{ele}^{ch} are the area-specific electronic resistance of the land and channel areas, respectively.

In the following calculations the ionic resistance for fully humidified Nafion® 117 [19] is used and the separately measured electronic resistance for the land and channel areas [9] are used. The results of the comparison of the iR-corrected polarization curves for the different flow field designs are shown in Figs. 5–7.

First, the results in Figs. 5–7 clearly show that the current density differences between the land and channel areas in the iR-corrected polarization curves are significantly smaller than those seen in the original polarization curves [8]. Secondly, there are obvious large differences in current density between the land and channel areas that still exist, especially for the cases with wider channels. For the case with narrow channels as shown in Fig. 7, the difference is not significant in the high cell potential region, similar to the results shown in the original polarization curves. This is caused by the higher indirect compression experienced by the channel area due to the very narrow channels, as explained previously [8].

The iR-corrected polarization curves show that the difference in total electrical resistance between the land and channel areas is an important factor in the observed difference in local current densities; however, it is not the only factor. As discussed above, the only other possible important factor is the local ECA. The result in ref. [7], reproduced here in Fig. 8, clearly shows that even at very low

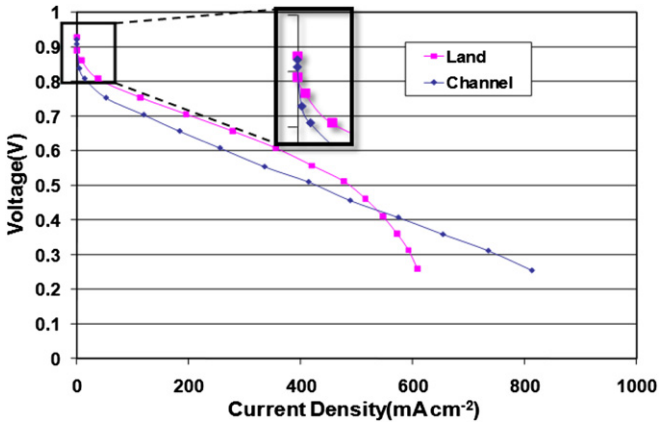

Fig. 8. Results of current density under land and channel in a PEM fuel cell. Cathode reactant is air, anode and cathode are fully humidified, and pressure is atmospheric [7].

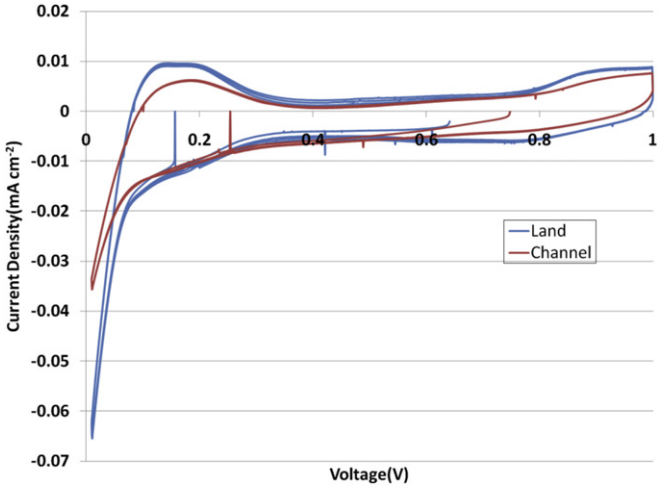

Fig. 10. cyclic voltammetry results for 3 mm land and 2 mm channel. The nitrogen purge rate is 200 sccm and the hydrogen flow rate is 200 sccm.

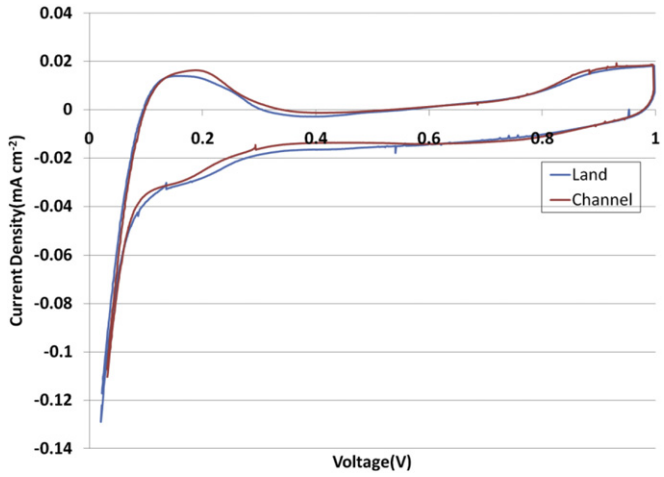

Fig. 11. ECA results for 1 mm land and 1 mm channel. The nitrogen purge rate is 200 sccm and the hydrogen flow rate is 200 sccm.

Table 2
ECA values for land and channel for the three flow fields.

Design	Channel width	Land width	M ($mg \cdot cm^{-2}$)	Land ECA ($cm^2 \cdot g^{-1}$)	Channel ECA ($cm^2 \cdot g^{-1}$)
A	2	3	0.4	7.04E + 05	5.51E + 05
B	2	2	0.4	8.44E + 05	5.68E + 05
C	1	1	0.4	8.59E + 05	7.71E + 05

current density, there exists a significant difference in local current density. Such a phenomenon indicates the possibility of a difference in local ECA between the land and channel areas.

For this reason the ECAs under the land and channel are measured separately in order to determine if there is indeed a difference in ECA and if such a difference is a significant factor in performance variations under the land and channel.

3.2. ECA under land and channel

The ECA under the land and channel areas are separately measured *in situ* following the procedure described in Section 2.1. The results of separately measured ECA for the flow field with a 2 mm land width and 2 mm channel width are shown in Fig. 9.

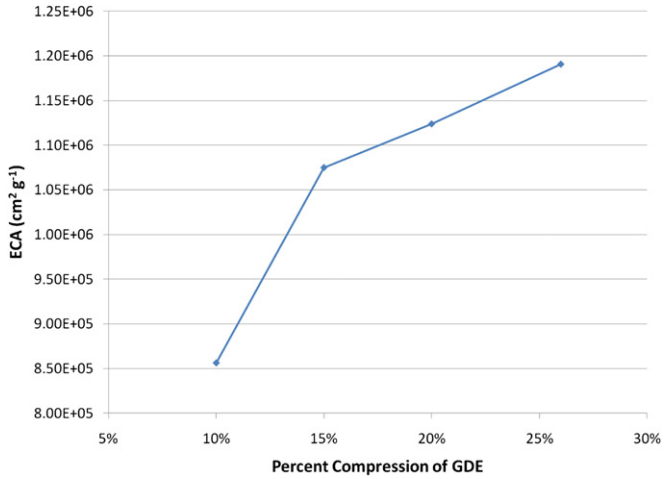

Fig. 12. Electrochemical active area as a function of GDE compression.

Table 3
Values of ECA at different cell compressions.

Percent compression	Manufacturer active area (cm^2)	Electrochemical active area ($cm^2 \cdot g^{-1}$)
10%	1.07	8.56E + 05
15%	1.07	1.07E + 06
20%	1.07	1.12E + 06
26%	1.07	1.19E + 06

Qualitatively it is immediately apparent that the land area has a significantly higher ECA than that of the channel area. The results for the flow fields with land width of 3 mm and the channel width of 2 and 2 mm land and 1 mm channel are shown in Figs. 10 and 11, respectively. The ECA values determined by Eq. (1) are given in Table 2. It is clear that the ECAs under the land areas are larger than those under the channel areas. These results indicate that it is possible that the compression under the land area is the cause of the higher ECAs. Note that the ECA under the channel area for the flow field with 1 mm channel is close to those under the land. This is most probably caused by the higher indirect compression experienced under the channel area when the channel is very narrow, as discussed in ref. [9].

3.3. ECA as a function of cell compression

In order to confirm if compression is indeed the cause of the higher ECA under the land areas, ECAs were measured at different compression levels for the land area. The flow field used is the one with 2 mm land and 2 mm channel and only the ECAs for the land area are measured at different compressions. The test fixture is shown in Fig. 4. The compression was varied from 10% to 26% in 5% increments. Below 10% compression is not possible to measure because 10% is the minimum amount required to create a proper seal for the fuel cell. The results of ECAs and different compressions are shown in Fig. 12. It is very clear that the ECA does in fact increase as the cell compression increases.

Table 3 shows the values of the ECA at different cell compressions. The largest increase occurs between 10% and 15% and then the increase in ECA begins to level off. These results, along with previous results, conclusively prove that the ECA increases with cell compression. Such an increase is likely due to the fact that as the

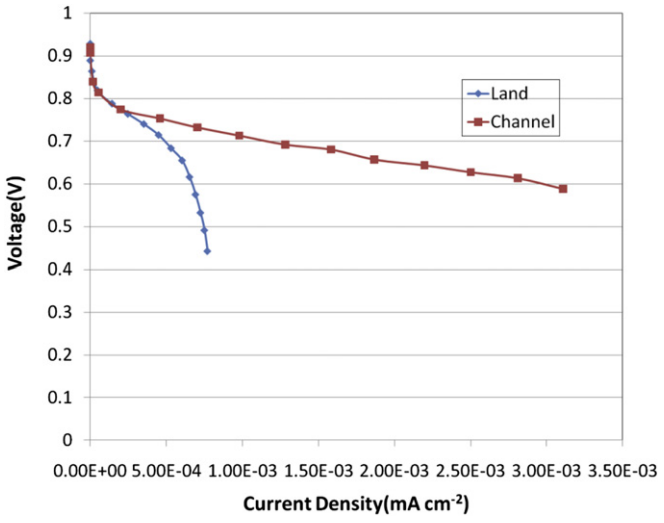

Fig. 13. Polarization curves with ECA-normalized current density and iR-corrected voltage for the flow field with 2 mm land and 2 mm channel.

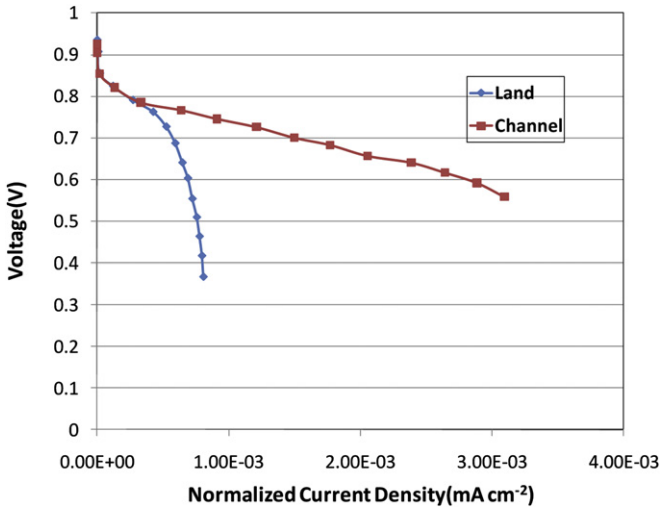

Fig. 14. Polarization plot of 3 mm land and 2 mm channel normalized by ECA and iR-corrected voltage.

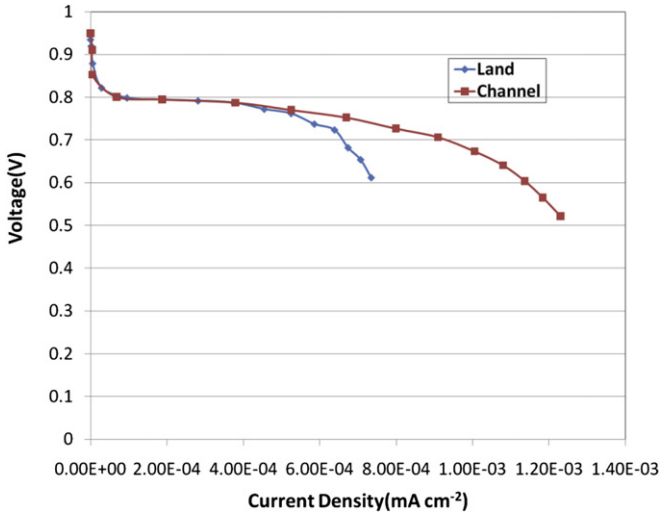

Fig. 15. Polarization plot of 1 mm land and 1 mm channel normalized by ECA and iR-corrected voltage.

compression increases, the contact between membrane material, platinum and carbon support in the catalyst layer improves, thereby increasing the total active surface area. These results indicate that the difference in ECA between land and channel is a major factor causing the difference in local current densities. That is, under the channel the GDE intrusion into the channel causes the channel region to have a lower compression, as shown in ref. [14]. The portion of the GDE under the channel experiences only indirect compression, that is, it is compressed only by the two portions of the land on either side, therefore, the larger the channel width the lower the indirect compression. This also explains why, when the channel width is reduced to 1 mm, the ECA increases.

3.4. ECA-normalized polarization curves

To further examine the effects of the difference in ECA, current densities in the iR-corrected polarization curves shown in Figs. 5–7 are normalized by the measured ECAs, and the resulting ECA-normalized and iR-corrected polarization curves are shown in Figs. 13–15, respectively. It is very clear that for all three cases in the low current density region, the ECA-normalized polarization curves for land and channel areas agree almost perfectly. Such a good agreement proves conclusively that the current density difference between land and channel areas in the high voltage region was mainly due to the difference in ECA. In the cell high voltage region, when the effects of electrical resistance and ECA are removed, the current densities under the land and channel are almost identical, thus there exists no other significant factors contributing to the difference in current densities.

Another very important issue is the true effect of mass transfer at the high current density/low cell potential region. In the high current density region, the ECA-normalized polarization curves shown in Figs. 13–15 are in extreme contrast to the original polarization curves shown in refs. [4] and [5] or the iR-corrected polarization curves shown in Figs. 5–7. By normalizing the current with the ECA values of the land and channel and by incorporating the iR-corrected voltage, the effect of the electrical resistance and ECA are removed. This means that the differences in performance shown are due strictly to the mass transport losses. It is clear from Figs. 13–15 that the true concentration losses for the land areas are much greater than can be seen from regular polarization curves. In addition, the effect of mass transfer for the land areas occurs at much lower current density compared to that of regular polarization curves. Furthermore it can be seen from Fig. 15 that there is noticeable concentration losses under the 1 mm channel at high current density region (e.g. at 1 mA cm^{-2}) in contrast to the other channel widths. The 1 mm channel experiences greater indirect compression compared to larger channel widths. These concentration effects can only be seen in the iR-corrected and ECA-normalized polarization curves. For the same channel widths, the one with wider land width may cause slightly higher indirect compression under the channel, thus a slightly higher performance, as seen in Figs. 13and 14 at 1 mA cm^{-2}.

4. Conclusion

Cyclic voltammetry measurements were successfully applied to separately measure the electrochemically active area (ECA) under the land and channel areas in a PEM fuel cell with a serpentine flow field. The following conclusions can be made based on the experimental results:

- In general, ECA is higher in the area under the land than that under the channel.
- The higher ECA under the land area is due to the higher compression from the flow field plate.
- As the channel width reduces, ECA under the channel increases due to the higher indirect compressions.
- The higher ECA under the land is the most important factor causing the higher current density, as compared to the channel area, within the high cell voltage region.
- ECA increases as a function of compression within the compression level used.
- The true concentration losses for the land areas are much greater compared to those seen in regular polarization curves.

References

[1] T. Zhou, H. Liu, Int. J. Trans. Phenomena 3 (2001) 177.
[2] T. Berning, D.M. Lu, N. Djilali, J. Power Sources 106 (2002) 284.
[3] U. Sukkee, C.Y. Wang, J. Power Sources 125 (2004) 40.
[4] D. Natarajan, T.V. Ngyuen, J. Electrochem. Soc. 148 (2001) A1324.
[5] S.A. Freunberger, M. Reum, J. Evertz, A. Wokaun, F.N. Buchi, J. Electrochem. Soc. 153 (2006) A2158–A2165.
[6] L. Wang, H. Liu, J. Power Sources 180 (2008) 365–372.

[7] A. Higier, H. Liu, J. Power Sources 193 (2009) 639–648.
[8] A. Higier, H. Liu, Int. J. Hydrogen Energy 35 (5) (2010) 2144–2150.
[9] A. Higier, H. Liu, Int. J. Hydrogen Energy 36 (2) (2011) 1664–1670.
1[0] Carter, et al., ECS Trans. 11 (1) (2007) 403–410.
[11] J. Wu, X.Z. Yuan, H. Wang, M. Blanco, J.J. Martin, J. Zhang, Int. J. Hydrogen Energy 33 (6) (2008) 1735–1746.
[12] T.R. Ralph, G.A. Hards, J.E. Keating, S.A. Campbell, D.P. Wilkinson, M. David, et al., J. Electrochem. Soc. 144 (1997) 3845–3857.
[13] M.A. Folgado, B. Gallardo, L. Daza, A.M. Chaparro, Int. J. Hydrogen Energy 34 (11) (2009) 4838–4846.
[14] I.A. Schneider, S. von Dahlen, A. Wokaun, G.G. Scherer, J. Electrochem. Soc. 157 (2010) 338–341.
[15] O'Harye, et al., Fuel Cell Fundamentals, John Wiley and Sons, New York, 2006.
[16] I. Nitta, T. Hottinen, O. Himanen, M. Mikkola, J. Power Sources 171 (2007) 26–36.
[17] I. Nitta, T. Hottinen, O. Himanen, M. Mikkola, Electrochem. Commun. 10 (2008) 47–51.
[18] J. Ge, A. Higier, H. Liu, J. Power Sources 159 (2006) 922–927.
[19] T.E. Springer, T.A. Zawodzinski, S. Gottesfeld, J. Electrochem. Soc. 138 (8) (1991) 2334–2342.